Electronic, magnetic, and optical properties of YMO_3 (M = Ti–Cu)

1997 J. Phys.: Condens. Matter 9 6267

(http://iopscience.iop.org/0953-8984/9/29/012)

J. Phys.: Condens. Matter **9** (1997) 6267–6277. Printed in the UK PII: S0953-8984(97)80340-2

Electronic, magnetic, and optical properties of YMO_3 (M = Ti–Cu)

S Bouarab†, A Vega† and M A Khan‡

† Departamento de Física Teórica, Universidad de Valladolid, E-47011 Valladolid, Spain

‡ IPCMS (UMR 46 CNRS), GEMME, 23, rue du Loess, F-63037 Strasbourg, France

Received 17 December 1996, in final form 10 April 1997

Abstract. The self-consistent *ab initio* energy bands of YMO_3 (M = Ti–Cu) are calculated by the linear-muffin-tin-orbitals (LMTO) method with local spin-density approximation (LSDA). For the non-magnetic phase, we have used cubic perovskite structure with one formula unit, whereas, for the magnetic phase, A-, C-, or G-type tetragonal or orthorhombic structures with higher numbers of formula units are considered. The non-magnetic energy bands predict the right tendencies as regards the existence of magnetism in the YMO_3 series. The calculated magnetic moments and magnetic phases are compared with those found by experimental measurements. These energy bands are further used to calculate the optical conductivity in the visible and ultraviolet regions. Only a few samples of YMO_3 have undergone optical conductivity measurements, with which our results are in comparatively good agreement. With the rest of the compounds, our theoretical calculations can be seen as precursors for future experiments.

1. Introduction

Earlier interest in the perovskite-type compounds was mainly due to their unusual magnetic and dielectric properties [1], and due to the observation of superconductivity in semiconducting samples of $SrTiO_3$ [2]. More recently, this interest was further enhanced by the discovery of high-T_c superconductivity in perovskite cuprate [3], and the observation of a huge negative magnetoresistance near room temperature, and the structural phase transition induced by an external magnetic field in $La_{1-x}D_xMnO_3$ (D = Ca, Sr, Ba) [4, 5]. These and other experimental observations [6–8] for $LaMO_3$ (M = Ti–Cu) have led to extensive theoretical energy band calculations with the local spin-density approximation [9–11]. The perovskite transition-metal oxides are considered to be highly correlated systems, and it is argued that the band theory is not appropriate for such compounds. Thus, to correct the deficiency of the LSDA energy band as regards giving the right insulating properties for some of the perovskites, LSDA + U theory [12, 13] is applied, where U is the intrasite Coulomb repulsion, and it is estimated in the framework of LSDA. However, in a recent article, Soloviev *et al* [14] have demonstrated that the localized picture for magnetic behaviour, where the appearance of a local moment is driven by the Coulomb interaction U, is in serious contradiction to the occurrence of an antiferromagnetic (AF) ground state for $LaMnO_3$. Moreover, it was shown that many aspects of the ground-state as well as single-electron excited-state properties of $LaMnO_3$ and other $LaMO_3$ compounds can be described satisfactorily in terms of LSDA energy bands [15–17].

As for YMO_3 compounds, there are many experimental measurements for their structural and magnetic properties available [18–28]. The optical conductivities of some YMO_3

0953-8984/97/296267+11$19.50

compounds (M = Ti, V, Co, Ni) were also measured [8, 29], but there has been almost no attempt to elucidate the physical properties of YMO_3 through energy bands. However, recently, Fujitani and Asano [30] have performed a full-potential band calculation of $YTiO_3$ with a distorted perovskite structure, to show that ferromagnetism and lattice distortion are necessary conditions for $YTiO_3$ to have a band gap at the Fermi level, but unfortunately without obtaining any conclusive evidence of this. Since most of the fundamental properties, and even the excited-state properties such as the optical conductivity of $LaMO_3$, are satisfactorily explained through the energy band calculations, we undertake in the present work the first systematic *ab initio* energy band calculations of YMO_3 (M = Ti, V, Cr, Mn, Fe, Co, Ni, and Cu) within the LSDA. In the absence of any systematic energy band calculation of YMO_3, we will compare the present results with those for $LaMO_3$ [10, 11], and observe the general trends as functions of the valency variation of M. The magnetic moments on transition metals will be compared with available experimental data, and lastly the optical properties for non-magnetic as well as for magnetic phases will be calculated, and they will be shown in a figure along with the available conductivity data [8, 29] for YMO_3 (M = Ti, V, Co, Ni). In a separate section we will discuss our results, and finally a general conclusion will be presented.

2. Energy bands

For the energy band calculations we use the linear muffin-tin orbitals with the atomic sphere approximation (LMTO-ASA), where the combined corrections are included [31]. These calculations are self-consistent, and the spin and exchange potentials are treated within the LSDA [32]. As usual, the initial potential is constructed with an isolated atomic charge distribution of neutral atoms by self-consistently solving the scalar relativistic Dirac equation [33]. The valence electrons considered for the initial charge density are $4d^15s^2$ for Y, $2s^22p^2$ for O, and 3d4s for M, with appropriate numbers of d and s electrons. The energies and eigenfunctions are determined, during the iterations for self-consistency, by the tetrahedron technique [34, 35], with 84 *k*-points uniformly distributed over the irreducible Brillouin zone.

Table 1. Lattice parameters and atomic sphere radii, in au, used in the calculation for cubic YMO_3 perovskites.

YMO_3	Lattice parameter	Atomic-sphere radii		
		Y	M	O
Ti	7.29 (reference [23])	3.99	2.31	1.76
V	7.22 (reference [19])	3.95	2.28	1.76
Cr	7.12 (reference [36])	3.88	2.22	1.79
Mn	7.25 (reference [22])	3.96	2.28	1.78
Fe	7.15 (reference [36])	3.90	2.24	1.78
Co	7.03 (reference [24])	3.81	2.18	1.76
Ni	7.09 (reference [21])	3.85	2.20	1.79
Cu	7.00[a]	3.67	2.07	1.78

[a]Due to the absence of experimental data for this compound, the lattice parameter of $YCuO_3$ has been determined by means of a total energy calculation.

The lattice parameters for all of these compounds are available through experimental measurements, except that for $YCuO_3$—this parameter was determined through total energy

calculation. The atomic sphere radii are determined in such a way as to satisfy the condition that the atomic sphere overlap is minimum (i.e. <15%). The lattice parameters and the corresponding atomic sphere radii are given in table 1. According to available experimental data, it seems that there is no uniform variation in lattice constants as M goes from Ti to Cu. This fact is revealed when we calculate the atomic sphere radii. It is noticeable that in all cases the largest and the smallest atomic spheres are those of Y and O respectively, and that the transition-metal spheres are intermediate, with radii $\simeq 2.19 \pm 0.12$ au.

Table 2. The number of electrons lost by the transition metal M (ΔQ^M/atom), the density of states at the Fermi energy ($\eta(E_F)$/YMO_3), the position of t_{2g} with respect to E_F ($E_{t_{2g}} - E_F$), and the gap between the M_d and O_{2p} bands calculated for the paramagnetic phase of the YMO_3 perovskites.

YMO_3	ΔQ^M/atom	$\eta(E_F)$/YMO_3	$E_{t_{2g}} - E_F$ (eV)	$E_{M_d} - E_{O_{2p}}$ (eV)
Ti	1.10	23.23	1.36	2.58
V	1.10	38.42	0.39	2.45
Cr	1.07	62.75	0.20	1.22
Mn	0.89	111.57	0.00	0.82
Fe	0.75	147.49	0.00	0.41
Co	0.74	11.52	−0.31	0.00
Ni	0.66	12.66	−1.09	0.00
Cu	0.83	13.96	−2.17	0.00

2.1. Non-magnetic phases

First we performed the band-structure calculation for YMO_3 cubic perovskite without spin polarization. The occupied energy bands are composed of three main contributions. The lowest band is mainly of oxygen (O_{2s}) origin. It lies about 2 Ryd below the Fermi level. The second band that is also completely occupied is of O_{2p} origin, with some other symmetries mixed in it. Around the Fermi level, we have the third band, mainly of M_{3d} origin, with a slight contribution from Y_d orbitals. We shall discuss the effect of M on these bands in the next section. In table 2 we present some pertinent physical quantities, such as the charge transfer, the DOS at the Fermi level, and the positions of different bands, for YMO_3 compounds in the paramagnetic phase.

2.2. Magnetic phases

Many of the YMO_3 compounds have been observed in magnetic phases, and in most of the cases they had orthorhombic structure with four formula units [20–28]. When the phase is AF, there are three possible structures according to the AF couplings in the (001) plane:

(i) with interplane AF coupling but intraplane F coupling—called A type;

(ii) the structure opposite to the A-type one, where the interplane coupling is F but the intraplane coupling is AF—this is called C type; and

(iii) with both couplings AF—this is called G type.

The A-type structure has two formula units, and is a tetragonal lattice with $a = b = a_0$ and $c = 2a_0$, where a_0 is the lattice parameter of the unit cubic perovskite. The C-type structure is also tetragonal with $a = b = \sqrt{2}a_0$ and $c = a_0$. Finally, the G-type structure may be orthorhombic ($a \neq b \neq c$) or tetragonal ($a = b = \sqrt{2}a_0$ and $c = 2a_0$), with four

Table 3. The calculated total energy differences per formula unit, in mRyd, of YMO_3 in different phases with respect to the most stable one. The magnetic moment obtained on the M ion is also given, in Bohr magnetons.

YMO_3	Structure	μ (μ_B)	ΔE (mRyd/YMO_3)
Ti	P		0.0
	F	0.03	0.0
V	AF-C	0.73	0.0
	AF-G	0.55	0.3
	AF-A	0.17	0.8
	P		2.0
Cr	AF-G	2.28	0.0
	AF-C	2.30	9.1
	F	1.95	27.8
	P		45.4
Mn	F	2.53	0.0
	AF-A	2.38	11.1
	AF-C	2.06	22.3
	AF-G	1.65	32.7
	P		48.9
Fe	F	1.74	0.0
	AF-C	0.90	19.1
	P		23.0

formula units. This last structure can also have only two formula units, with two face-centred-cubic (fcc) sublattices, where two inequivalent 3d metals with spin up and down replace Na and Cl in the NaCl structure. This facilitates the energy band calculation, due to the smaller number of atoms (ten) that there are per unit cell [11].

We have performed the magnetic phase energy band calculations for YMO_3 only for M = Ti, V, Cr, Mn, and Fe. This is because the densities of states (DOS) at the Fermi level for the compounds with M = Co, Ni, and Cu are very low in the paramagnetic phase, and also experimentally there is no strong evidence of magnetism in these compounds. For magnetic systems, we have considered some other possible phases besides the most stable one. All of the magnetic phases are treated as having two formula units. In figure 1 we present the total DOS for the most stable structures. In table 3 we give the charge transfer on the transition metal M, the magnetic moment per M atom in different phases, and also the total energy difference with respect to the most stable phase. The total energies calculated by the LMTO method have a limit of precision. Usually, these values are correct to the order of mRyd [31]. These results will be discussed shortly.

2.3. Optical conductivity

Once the energy bands are obtained, one can easily calculate the interband optical conductivity through [11]

$$\sigma_1(\omega) = \frac{1}{\pi^2\omega}\sum_{n,n'}\int_{\mathrm{BZ}}\frac{|\boldsymbol{e}\cdot\boldsymbol{P}_{nn'}(\boldsymbol{k})|^2}{|\boldsymbol{\nabla}\omega_{nn'}(\boldsymbol{k})|}\,\mathrm{d}\boldsymbol{S}_k \tag{1}$$

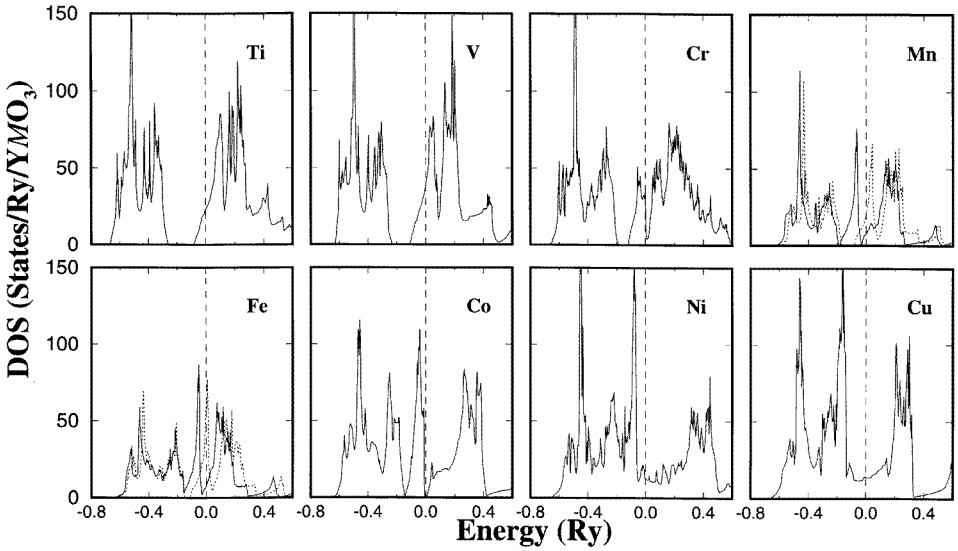

Figure 1. Densities of states of YMO_3 (M = Ti–Cu) obtained for the most stable magnetic structures. The dotted lines in the Fe and Mn ferromagnetic DOS represent the minority-spin contribution.

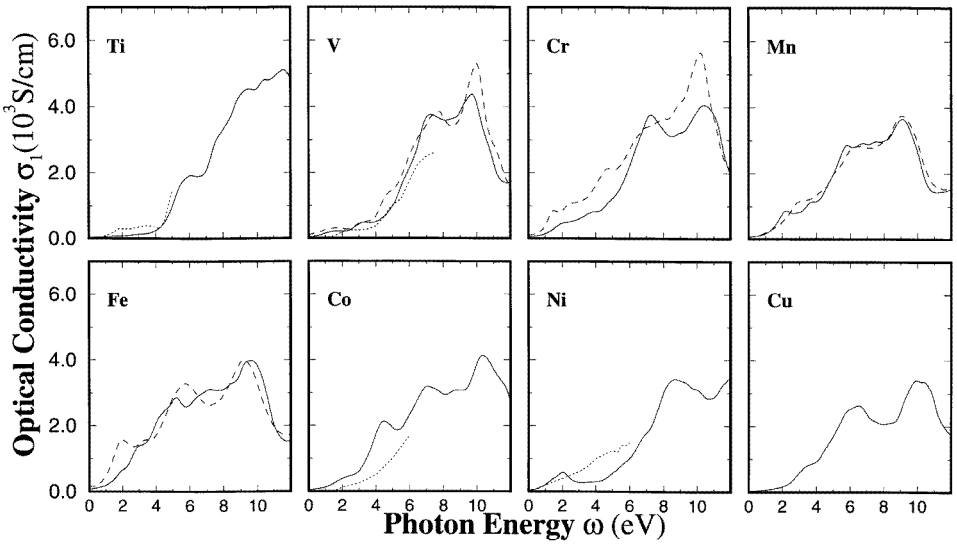

Figure 2. The optical conductivity $\sigma_1(\omega)$ of YMO_3 (M = Ti–Cu) calculated for the paramagnetic phase (thick solid line), and for the G-type AF phase for Cr, for the C-type AF phase for V, and for the ferromagnetic phase for Mn and Fe (dashed lines). The thin dotted lines show the experimental data of Arima *et al* [8] for Ti, Co, and Ni, and the data obtained by Kasuya *et al* [29] for V.

where ω is the photon energy (Ryd), $\boldsymbol{e}$ is the unit vector of light propagation, and $P_{nn'}(\boldsymbol{k})$ is the dipole matrix element connecting the initial $|n\boldsymbol{k}\rangle$ and final $|n'\boldsymbol{k}\rangle$ states with eigenvalues $E_n(\boldsymbol{k})$ and $E_{n'}(\boldsymbol{k})$, respectively. The integration is performed by the

tetrahedron technique [34, 35] over the Brillouin zone, where the constant surface energy is $S = \{\boldsymbol{k}; E'_n(\boldsymbol{k}) - E_n(\boldsymbol{k}) = \omega_{nn'}(\boldsymbol{k}) = \omega\}$. The above expression (1) is written in atomic units. Thus, our calculated optical conductivity will be in units of Ryd, but for comparison with experimental data we have converted it to the usual S cm^{-1}. In figure 2 we present our calculated results for the paramagnetic phase for all of the compounds and for the most stable magnetic phases, along with the experimental data for M = Ti, V, Co, and Ni.

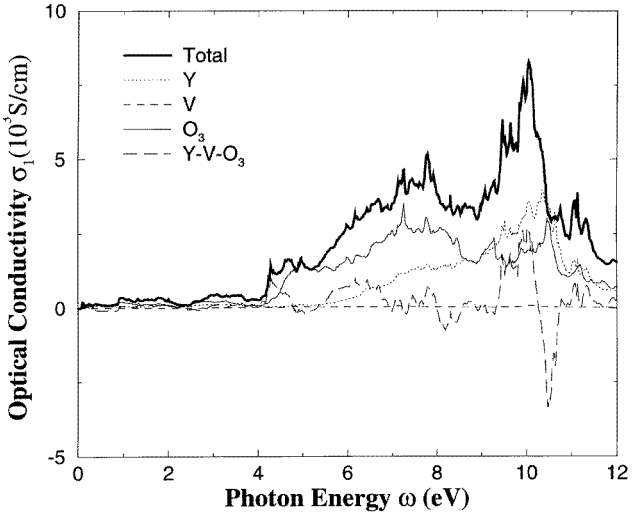

Figure 3. The different contributions to the optical conductivity $\sigma_1(\omega)$ of YVO_3 in the C-type AF phase: the total contribution (thick solid line), the contribution of the Y atom (dotted line), the contribution of O atoms (thin solid line), the contribution of the TM element V (dashed line), and the cross-contribution Y–V–O_3 (chain line). The results are reported without the Lorentzian broadening.

To check the origin of the different atomic contributions to $\sigma_1(\omega)$, one can also write

$$\sigma_1(\omega) = \sigma_1^{(Y)}(\omega) + \sigma_1^{(M)}(\omega) + \sigma_1^{(O_3)}(\omega) + \sigma_1^{(Y-M-O_3)}(\omega) \tag{2}$$

where $\sigma_1^{(X)}(\omega)$ is the contribution from atomic sphere X, and the last term is the term for the interference between the three chemical species, which can be either positive or negative. Figure 3 shows the different contributions to the optical conductivity as expressed in equation (2) for YVO_3 in the C-type AF phase.

3. Discussion

3.1. Electronic structure

When compared with that of $LaMO_3$, the electronic structure of YMO_3 is seen to look somewhat similar in the low-energy range. For YMO_3 also, the lowest occupied band is of O_{2s} origin, about 2 Ryd below the Fermi level (E_F), as it was in the case of $LaMO_3$. The next occupied band is of O_{2p} origin with a small percentage of M_{3d} origin. This percentage keeps on increasing as we go from Ti to Cu, but it never exceeds 30%, and it shifts toward E_F as M increases (i.e. goes from Ti to Cu). Lastly, around the Fermi level we have mainly an M_{3d} band with some mixing of Y_{4d}. The Y_{4d} band is centred at around 0.2 Ryd above the Fermi level, and remains almost fixed. The M_{3d} part of the band moves toward lower

energy, and for M $\geqslant$ Co merges into the large O_{2p} band (table 2, column 5). The Y_{4d} part of the band remains almost fixed at its centre. The M_{3d} band is split into t_{2g} and e_g bands. The t_{2g} part is well separated from the main band, whereas e_g is mixed with and enlarged by the Y_{4d} band. At the beginning of the series, the t_{2g} band falls on the higher-energy side of E_F (i.e. $E_{t_{2g}} > E_F$). As M increases, this peak moves towards lower energy, and when M = Mn and Fe, it falls right at the Fermi level, and then it keeps on moving away from E_F towards lower energy (table 2, column 4). The movement of the t_{2g} level entails corresponding changes in the density of states at the Fermi level (table 2, column 3). In all cases, the M atomic sphere loses some charge in favour of the other two, but mainly in favour of O. Table 2 indicates some general tendencies of the electronic properties of YMO_3 perovskites in the paramagnetic phase.

3.2. Magnetic properties

From the DOS at E_F in the paramagnetic phase, one can deduce some pertinent information concerning the magnetism in the YMO_3 system. $YMnO_3$ and $YFeO_3$ are the most favourable compounds for magnetism. $YCrO_3$ is also a good candidate. $YTiO_3$ and YVO_3 may have some weak magnetic moments, whereas the remaining three metals considered (M = Co, Ni, Cu) could be excluded as regards the existence of magnetism. Experimentally, there are no convincing data on the magnetic structure of the last three compounds, except for $YNiO_3$, which is found to have a G-type AF structure with a distorted crystal [21]. We did try a simple G-type AF ordering with cubic structure for this compound, but the self-consistency always gives a 0.00 μ_B magnetic moment at the Ni site. Demazeau *et al* [21] do not give any estimate of the magnetic moment at the Ni site. For M = Co and Cu, only the paramagnetic phase was studied. The results concerning the magnetic phases are given in table 3. In figure 1 we present the total DOS for all of the compounds in their most stable structures.

According to the total energy calculation, the P and F phases are degenerate states for $YTiO_3$ with a very weak magnetic moment (0.03 μ_B per Ti atom) in the F phase. The measured value [18] is quite high (0.84 μ_B). A previous full-potential calculation [30] for a distorted perovskite structure also gives a small (0.08 μ_B) magnetic moment on Ti.

YVO_3 is found to be more stable in the AF phase than in the P phase. But the difference of energies between different AF phases is so small (i.e. <mRyd) that their relative stabilities may be considered to be the same. The C-type AF phase has a magnetic moment of 0.73 μ_B. Other magnetic phases, according to the band theory, give even smaller moments (see table 3). The G-type and A-type AF phases with magnetic moments of 0.55 and 0.17 μ_B have an energy slightly higher than that of the AF-C phase. Kawano *et al* [19] have studied this compound by means of neutron scattering. They conclude that the static moment which contributes to the long-range order when extrapolated to $T = 0$ K is less than 1.6 μ_B.

When M = Cr, the magnetic moment increases to 2.28 μ_B, and the G-type AF phase is the most stable one. The C-type AF ordering of $YCrO_3$ has a somewhat higher moment (i.e. 2.3 μ_B), but on the other hand also has a higher total energy. There are no experimental data concerning the magnetic moment on Cr in this compound.

The cubic perovskites $YMnO_3$ and $YFeO_3$ are found with minimum total energies in the F phase, with magnetic moments of 2.53 and 1.74 μ_B respectively. According to Quezel *et al* [22], orthorhombic $YMnO_3$ is reported to order antiferromagnetically with helical structure, with a magnetic moment of 3.1 μ_B. We do have a possible A-type solution with 2.38 μ_B on the Mn ion but a total energy 11.1 mRyd higher than that in the F phase. $YFeO_3$ has a magnetic moment of 1.74 μ_B in the A-type AF phase and 0.90 μ_B in the C-type AF

phase. Our values of the magnetic moments for either phase are much smaller than the only available measured value [28], namely 4.1 μ_B.

3.3. Optical conductivity

The self-consistent energy bands for different phase structures are further used to calculate the interband conductivities. For this purpose we use expression (1). For a comparison with experimental data, the $\sigma_1(\omega)$ obtained through (1) is further broadened by a Lorentzian with a lifetime τ (i.e. $\tau^{-1} = 2$ mRyd). For all of the compounds YMO_3, we give $\sigma_1(\omega)$ for the paramagnetic phase and also for the most stable magnetic phase. Along with these theoretical curves, we also show in figure 2 the available experimental data for a few of these compounds (those with M = Ti, V, Co, and Ni).

For $YTiO_3$, in the low-energy range, the interband transition is almost absent. At about 3.0 eV, the conductivity starts increasing, and a first peak is observed at $\simeq$6.0 eV. $\sigma_1(\omega)$ increases gradually, with structures at 7.6, 9.2, 10.5, and 11.6 eV. The first peak at 6.0 eV appears when the interband transitions between the higher-energy parts of O_{2p} and t_{2g} take place. For higher-energy transitions, more and more high-density peaks in occupied and empty states become active. The origin of all of the high-energy peaks can be easily traced back to the respective high-density regions in figure 1. The experimental data [8] are very close to the theoretical curve.

In the case of YVO_3, in the paramagnetic phase, there is a small structure at $\simeq$3.1 eV; otherwise $\sigma_1(\omega)$ is almost flat in the low-energy range. The first peak appears at $\simeq$7.2 eV, and another one appears at about 10.0 eV. $\sigma_1(\omega)$ for the most stable phase, AF-C (or AF-G since the two phases can be considered as degenerate), is almost the same as for the P phase, except that the high-energy peaks are somewhat shifted to higher energies, and a new shoulder-like structure appears at about 4.6 eV. This new structure is also observable in the experimental data [29].

In the paramagnetic phase of $YCrO_3$, there are some small structures in the low-energy range, but the important peaks are at $\simeq$6.9 eV (A) and 10.4 eV (B). For the G-type AF phase the peak B becomes more pronounced at 10.2 eV, and peak A changes into a shoulder-like structure. Moreover, some new observable structures appear in the low-energy range, at 1.4 and 4.6 eV.

The two perovskites $YMnO_3$ and $YFeO_3$ are at their most stable in the F phase according to the total energy calculation. The optical conductivities in the P and F phases for either compound are similar, with some relative shifts of the conductivity peaks for the F phase as compared to the positions of those for the P phase. To illustrate the effect of spin polarization on the conductivity $\sigma_1(\omega)$ in $YMnO_3$, we show in figure 4 the contribution of majority (+) and minority (−) spins. It becomes evident that the two types of spin contribute almost equally, except that $\sigma_1^+(\omega)$ is slightly more important in the low-energy range (i.e. where $\omega < 4.0$ eV), whereas in the high-energy range it is $\sigma_1^-(\omega)$ which becomes somewhat more dominant.

In the cubic P phase, $YCoO_3$ has a very small structure at $\simeq$1.8 eV, then a prominent peak at $\simeq$4.8 eV, and lastly one at $\simeq$11.3 eV. In between these two high-energy peaks, there are some small structures. In figure 2 we do not present the results for this cubic structure, but only those for the orthorhombic structure with the experimental lattice parameters [24], where the situation is quite different. The small shoulder-like structure at 1.8 eV in the cubic P phase disappears, but prominent structures at 4.4, 7.1, and 10.3 eV are observed. The experimental $\sigma_1(\omega)$ is almost a monotonically increasing curve until 6.0 eV is reached. Unfortunately, there is no structure in the low-energy range at 4.4 eV, as

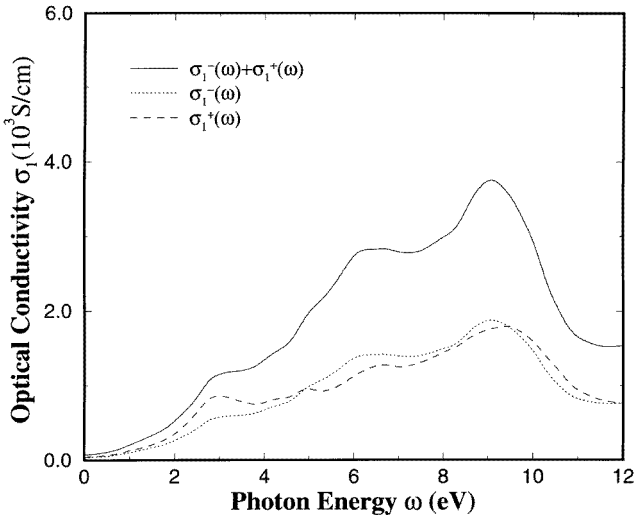

Figure 4. The contribution of the majority (dashed line) and minority spins (dotted line) to the total optical conductivity of $YMnO_3$ perovskite in the F phase.

obtained theoretically. It is possible that the experimental lifetime broadening is much bigger than 0.02 mRyd. Otherwise, the experimental curve has a better agreement with the orthorhombic than the cubic P phase.

The compounds $YNiO_3$ and $YCuO_3$ are found to be stable in the usual cubic P structure. In $YNiO_3$ there is a small structure at 2.0 eV and then a broad peak at 8.5 eV. The low-energy peak (i.e. that at 2.0 eV) is not observed experimentally. In the case of $YCuO_3$, a shoulder at 3.2 eV, then two broad peaks centred at 6.3 and 10.0 eV are obtained. The origin of all of the peaks obtained through interband transitions can be easily traced back to the high-density regions in the DOS curves, as in the case of $YTiO_3$.

To obtain the exact contributions of different origins as expressed by equation (2), we have considered as an example the case of YVO_3. In figure 3, we show the different contributions $\sigma_1^{Y}(\omega)$, $\sigma_1^{V}(\omega)$, and $\sigma_1^{O_3}(\omega)$, and the cross-term $\sigma_1^{Y-V-O_3}(\omega)$. From figure 3, it is apparent that the main contribution is from oxygen atomic spheres, particularly in the low-energy range. Then the contribution from the Y atomic sphere becomes somewhat more important in the energy range >8.0 eV. The V atomic sphere makes no direct contribution to the optical conductivity. In the optical properties, the transition metals M play an indirect role in changing the local density of states in the Y and O atomic spheres, which provide the main contributions to the optical conductivity.

4. Summary

A systematic theoretical study of the electronic, magnetic, and optical properties of YMO_3 (M = Ti–Cu) perovskites is presented. For the electronic properties, three different types of chemical species have their predominant contributions in different energy ranges. The occupied states are mainly of oxygen origin; the empty states in the high-energy region are on the other hand mainly of Y origin, whereas the states around the Fermi level are dominated by the transition metals (M). None of these states is purely of one particular origin—they are always mixed with some other states originating from different chemical

species and having different symmetries. The magnetic properties originate from the local DOS of the transition metals. No magnetism is induced either on O or on Y ions.

The present work gives values for the magnetic moments on the M site that are much smaller than the few available experimental data. For the systems with M = Ti, V, Mn, and Fe, we have in each case a single experimental datum. For $YTiO_3$ we obtain a very small magnetic moment on Ti as compared to that obtained experimentally. This is certainly not because we have not considered the distorted structure, since Fujitani and Asano [30] have used a distorted structure in their full-potential energy band calculation, and still obtained a value that was only one tenth of the experimental value for the magnetic moment on Ti. For YVO_3 (0.73 μ_B), $YMnO_3$ (2.53 μ_B), and $YFeO_3$ (1.74 μ_B), we do obtain high magnetic moments, but still not as high as those measured experimentally. This may not simply be the fault of the LSDA, since a similar calculation for the same transition-metal elements in $LaMO_3$ gives magnetic moments of 1.22, 3.00, and 4.00 μ_B respectively when M = V, Mn, and Fe [11]. On the other hand, it is well known that a small change in the lattice parameter may appreciably change the magnetic properties [37]. But we think that more precise measurements are necessary before making any further theoretical attempt to obtain higher magnetic moments.

For optical conductivity, M plays an indirect role. The interband transitions are due to oxygen and yttrium atoms. These tendencies were also observed in previous work [11] on $LaMO_3$. In the present work, the available experimental data are compared with the calculated results, and a satisfactory agreement is found. Unfortunately, the compounds YMO_3 have not been as extensively studied by the experimentalists as $LaMO_3$. More experimental studies, particularly in the domain of interband transitions, will be most welcome.

Acknowledgments

We gratefully acknowledge useful discussions with Professor L C Balbás. This work was supported by the DGICYT (Grant PB95-0720-CO2-O1), the Junta de Castilla y León (Grant VA58/93) from Spain, the TRM-Network (Interface Magnetism), and NATO (CRG 960975). MAK and SB would like to thank the Ministerio de Educación y Ciencia (Spain) for a Sabbatical grant and financial support, respectively. One of us (MAK) would like to thank the members of the Departamento de Física Teórica, Atómica, Molecular y Nuclear, Universidad de Valladolid, for their kindness and hospitality during his four months' sabbatical leave.

References

[1] Goodenough J B and Lango J M 1970 *Landolt–Börnstein Tabeller* ed K H Hellwege and A M Hellwege (Berlin: Springer)
[2] Schooley J F, Hosler W R and Cohen M L 1964 *Phys. Rev. Lett.* **12** 474
[3] Bednorz J G and Müller K A 1986 *Z. Phys.* B **64** 189
[4] von Helmolt R, Wecker J, Holzapfel B, Shultz L and Samwer K 1993 *Phys. Rev. Lett.* **71** 2331
[5] Urushibara A, Arima T, Asamitsu A, Kido G and Tokura Y 1995 *Phys. Rev.* B **51** 14 103
[6] Crandles D A, Timusik T, Garret J D and Greedan J E 1994 *Phys. Rev.* B **49** 16 207
[7] Sreedhar K, Honig J M, Darwin M, McElfresh M, Shand P M, Xu J, Crooker B C and Spalek J 1992 *Phys. Rev.* B **46** 6382
[8] Arima T, Tokura Y and Torrance J B, 1993 *Phys. Rev.* B **48** 17 006
[9] Sarma D D, Shanthi N, Barman S R, Hamada N, Sawada H and Terakura K 1995 *Phys. Rev. Lett.* **75** 1126
[10] Pari G, Mathi Jaya S, Subramoniam G and Asokamani R 1995 *Phys. Rev.* B **51** 16 575
[11] Bouarab S, Vega A and Khan M A 1996 *Phys. Rev.* B **54** 11 271

[12] Anisimov V I, Zaanen J and Andersen O K 1991 *Phys. Rev.* B **44** 943
[13] Soloviev I V, Dederichs P H and Anisimov V I 1994 *Phys. Rev.* B **50** 16 861
[14] Soloviev I V, Hamada N and Terakura K 1996 *Phys. Rev.* B **53** 7158
[15] Sarma D D, Shanthi N and Mahadevan P 1996 *Phys. Rev.* B **5** 1622
[16] Pickett W E and Singh D J 1996 *Phys. Rev.* B **53** 1146
[17] Soloviev I V, Hamada N and Terakura K 1996 *Phys. Rev. Lett.* **76** 4825
[18] Goral J P, Greedan J E and MacLean D A 1982 *J. Solid. State Chem.* **43** 244
[19] Kawano H, Yoshizawa H and Ueda Y 1994 *J. Phys. Soc. Japan* **63** 2857
[20] Cintolesi F, Corti M, Rigamonti A, Rossetti G, Ghigna P and Lascialfari A 1996 *J. Appl. Phys.* **79** 1
[21] Demazeau G, Marbeuf A, Pouchard M and Hagenmuller P 1971 *J. Solid State Chem.* **3** 582
[22] Quezel S, Rossat-Mignod J and Bertaut F F 1974 *Solid State Commun.* **14** 941
[23] MacLean D A, Ng Hok-Nam and Greedan J E 1979 *J. Solid State Chem.* **30** 35
[24] Kappatsch A, Quezel-Ambrunaz S and Sivardière J 1970 *J. Physique* **31** 369
[25] Belov K P, Kadomtseva A M, Krynetskii I B, Ovchinnikova T L, Ronami G M and Timofeeva V A 1972 *Sov. Phys.–Solid State* **14** 1306
[26] Pauthenet R and Veyret C 1970 *J. Physique* **31** 65
[27] Jacobs I S, Barne H F and Levinson L M 1971 *J. Appl. Phys.* **42** 1631
[28] Treves D 1965 *J. Appl. Phys.* **36** 1033
[29] Kasuya M, Tokura Y, Arima T, Eisaki H and Ushida S 1993 *Phys. Rev.* B **47** 6197
[30] Fujitani H and Asano S 1995 *Phys. Rev.* B **51** 2098
[31] Andersen O K 1975 *Phys. Rev.* B **12** 3060
Skriver H L 1984 *The LMTO Method* (Berlin: Springer)
[32] von Barth U and Hedin L 1972 *J. Phys. C: Solid State Phys.* **5** 31
[33] Desclaux J B 1975 *Comput. Phys. Commun.* **2** 31
[34] Jepsen O and Andersen O K 1971 *Solid State Commun.* **9** 1763
[35] Lehman G and Taut M 1972 *Phys. Status Solidi* b **54** 469
[36] Villars P and Galvert L D 1985 *Pearson's Handbook of Crystallographic Data for Intermetallic Phases* (Metals Park, OH: American Society for Metals)
[37] Moruzzi V L and Marcus P M 1992 *Phys. Rev.* B **45** 2934